Supporting Information

Endo et al. 10.1073/pnas.1710837114

SI Materials and Methods

Mice. Three types of mice were used: WT (C57BL/6NTac), *Dmc1*-deficient (B6.Cg-Dmc1^{tm1Jcs}/JcsJ) (50), and *Spo11*-deficient (B6-129X1 Spo11^{tm1Mjn}) (52). C57BL/6NTac mice were purchased from Taconic Biosciences. *Dmc1*-deficient mice (strain name B6.Cg-Dmc1^{tm1Jcs}/JcsJ) were purchased from The Jackson Laboratory and backcrossed to C57BL/6NTac mice for at least 15 generations. Heterozygous animals were mated to generate *Dmc1*-deficient homozygotes. *Dmc1* genotypes were assayed by PCR, using the protocol provided by The Jackson Laboratory. *Spo11*-deficient mice (strain name B6-129X1 Spo11^{tm1Mjn}) were purchased from The Jackson Laboratory. This line was on a mixed background, having been mated to 129S4/SvJae and C57BL/6N. Heterozygous animals were mated to generate *Spo11*-deficient homozygotes. *Spo11* genotypes were assayed by PCR, using the protocol provided by The Jackson Laboratory.

Identification of the Stages of the Seminiferous Cycle. Seminiferous stages were determined using hematoxylin and periodic acid-Schiff (PAS)-stained cross sections, according to morphological criteria (10, 62). In brief, the 12 stages were identified primarily based on the first 12 steps of spermatid development. When the patterns of germ cell associations were changed after RA or WIN18,446 treatment, the stages were identified according to spermatid development.

Chemical Treatments. For RA injection experiments, adult mice received i.p. injections of 100 μL of 7.5 mg/mL all-*trans* RA (Sigma-Aldrich) in 16% DMSO-H_2O, and young (P15) mice received i.p. injections of 10 μL/g body weight of 5 mg/mL all-*trans* RA in 10% DMSO-H_2O. For WIN18,446 injection experiments, adult mice received i.p. or s.c. injections of 100 μL of 20 mg/mL WIN18,446 (sc-295819A; Santa Cruz Biotechnology) in 16% DMSO-H_2O, and young (P2 to P14) mice received s.c. injections of 10 μL/g body weight of 10 mg/mL WIN18,446 in 5% DMSO-H_2O. For 5-bromo-2-deoxyuridine (BrdU) incorporation experiments, mice received i.p. injections of 10 μL/g body weight of 10 mg/mL BrdU (Sigma-Aldrich) in PBS, 4 h before they were killed. For 5-ethynyl-2′-deoxyuridine (EdU) incorporation experiments, mice received i.p. injections of 5 μL/g body weight of 4 mg/mL EdU (Thermo Fisher Scientific) in PBS, 4 h before they were killed. For hydroxyurea (HU) cell depletion assays, mice received i.p. injections of 50 μL of 140 mg/mL HU (Spectrum Chemical) in PBS at 6-h intervals for a total of 36 h.

Immunostaining on Testis Sections. Testes were fixed overnight in Bouin's solution at room temperature (for colorimetric detection) or in 4% (wt/vol) paraformaldehyde (PFA) at 4 °C (for fluorescence detection), embedded in paraffin, and sectioned at 5 μm thickness. Slides were dewaxed, rehydrated, and heated in 10 mM sodium citrate buffer (pH 6.0) and blocked for 30 min. Slides were incubated with primary antibody for 1 to 2 h at room temperature, washed with PBS, incubated with the secondary antibody for 30 min at room temperature, and washed with PBS. Detection was fluorescent or colorimetric. Antibodies and incubation conditions are listed in Dataset S1.

For colorimetric detection, samples were incubated with rabbit ImmPress peroxidase reagent (Vector Labs) or with anti-rat biotinylated IgG (BA4001; Vector Labs) and VECTASTAIN HRP reagent (Vector Labs), and developed using a DAB peroxidase substrate kit (Vector Labs). Samples were then counterstained with Mayer's hematoxylin (or He-PAS), dehydrated, and mounted with Permount (Fisher Scientific).

For fluorescence detection, samples were incubated with fluorescent-conjugated donkey secondary antibodies (Jackson ImmunoResearch Laboratories) at a concentration of 1:200 and then mounted with VECTASHIELD mounting media with or without DAPI (Vector Labs). For EdU detection, slides were stained using a Click-it EdU Alexa Fluor 488 imaging kit (C10337; Thermo Fisher Scientific) according to the manufacturer's protocol.

Nuclear Spreads of Spermatocytes. Testes were dissected to obtain single cells, including spermatocytes, as previously described (8). Seminiferous tubules were teased apart with forceps, minced, and pipetted repeatedly in PBS. Cells were pelleted and resuspended once in PBS and twice in hypotonic solution (0.5% sodium chloride in H_2O). Cells were pelleted, resuspended in 100 mM sucrose (in H_2O), and placed on poly-L-lysine–coated slides. The slides were then fixed in 1% PFA (containing 0.15% Triton X-100), kept in a humid chamber at room temperature for 2 h, washed in 0.4% (vol/vol) Photoflo (Kodak) for 1 min, and air dried. These slides were stored at −80 °C before use. For immunostaining, slides were brought to room temperature and washed with PBS.

Single-Molecule Fluorescent in Situ Hybridization. Probe design, synthesis, and coupling were as previously described (47, 63). Testes were fixed in 4% (wt/vol) PFA for 2 h at 4 °C, incubated overnight in 30% sucrose/4% PFA/PBS at 4 °C, and then embedded in O.C.T. compound (Sakura Finetek). Frozen blocks were sectioned at 8 μm thickness and dehydrated overnight in 70% (vol/vol) ethanol at 4 °C. Hybridization was performed as previously described (47, 63). Counting of individual mRNA particles, image stitching, and data analysis were performed using custom Matlab software as previously described (47, 63). In all experiments, germ cell types were identified with DAPI nuclear staining, and cell borders were visualized using overexposed images (Fig. S7*B*). To count the number of smFISH punctate signals per Sertoli cell, signals in germ cells were excluded from the image area, and the remaining signals were normalized by Sertoli cell numbers. All smFISH probes used to visualize transcripts were purchased from LGC Biosearch Technologies. The probes for *Gapdh* were conjugated to Quasar 570 (SMF3002-1; LGC Biosearch Technologies) or Quasar 670 (SMF3015-5; LGC Biosearch Technologies). The probes for *Stra8* were conjugated to Quasar 610, and their sequences are as previously described (65). The probes for *Aldh1a1*, *Aldh1a2*, and *Aldh1a3* were conjugated to Quasar 670, and their sequences are listed in Dataset S2.

Absolute Quantification of RA Levels. Sample preparation and quantification of RA levels were performed according to a published protocol (64). To avoid chemical degradation, testes and testicular extracts were handled under yellow lights using exclusively glass or stainless steel containers, pipettes, and syringes. Testes were collected and homogenized by hand in ground glass homogenizers on ice in 1 mL of saline (0.9% NaCl). All-*trans* RA was extracted as described (64), adding 10 μL of 1 μM all-*trans* RA-d_5 (R250202; Toronto Research Chemicals) as internal standard to each tissue sample. The dried extracts were resuspended in 100 μL of acetonitrile, and 15 μL were injected for liquid chromatography/mass spectrometry (LC/MS) analysis. The chromatographic gradient utilized an Ascentis RP-Amide column, 15 cm × 2.1 mm with 3-μm particle size (Sigma-Aldrich), exactly as described (64). After chromatographic separation,

the column eluate was introduced into a QExactive orbitrap mass spectrometer (Thermo Fisher Scientific) equipped with an IonMax source and a HESI II source. The mass spectrometer was operated in positive ionization mode with the spray voltage set to 3.0 kV, the heated capillary held at 275 °C, the HESI probe held at 350 °C, and the S-lens RF level set to 40. The sheath gas flow was set to 40 units, the auxiliary gas flow was set to 15 units, and the sweep gas flow was set to 1 unit. The MS data were acquired in multiplexed targeted selected ion monitoring (tSIM) mode for all-*trans* RA at 301.2162 *m*/*z* and all-*trans* RA-d_5 at 306.2476 *m*/*z*, using a mass window of 1.0 *m*/*z*, a resolution of 70,000, the automatic gain control (AGC) target at 2e5, and the maximum injection time at 250 ms. Peak integration for all-*trans* RA and all-*trans* RA-d_5 was performed with XCalibur QuanBrowser 2.2 (Thermo Fisher Scientific) using a 5-ppm mass tolerance. For absolute quantification of all-*trans* RA levels, a calibration curve of 1 nM to 10 μM all-*trans* RA in acetonitrile, in semilog dilutions, containing 100 nM all-*trans* RA-d_5 as internal standard, was analyzed in parallel with each biological sample batch. External mass calibration was performed using the standard calibration mixture every 7 d.

SI Results

Sperm Release and Spermatid Elongation After WIN18,446 Treatment. To examine the primary effect of RA on the two postmeiotic transitions, we assessed the near-term consequences of treating male mice with WIN18,446 for only 2 or 4 d. Such treatment did not completely block either sperm release or spermatid elongation (Fig. 2 *B*–*E* and Fig. S2 *B*–*F*). This may be due to low levels of RA persisting in testes after WIN18,446 treatment. Indeed, we previously observed (22) that WIN18,446 treatment daily for 4 d did not completely block meiotic initiation, indicating that short-term WIN18,446 treatment does not completely eliminate RA. More to the point, in Fig. S3*A*, we demonstrate that 8 or 14 d of WIN18,446 treatment results in a severe block of spermatid elongation (and sperm release) and resultant apoptosis; at 21 d, nearly all tubules containing spermatids showed a complete block of spermatid elongation, and resultant apoptosis. These time-dependent effects of WIN18,446 treatment mirror the time-dependent effects of a vitamin A-deficient diet, which takes 14 to 16 wk for male mice (following treatment of the mother for 4 wk) to achieve a complete block of spermatogonial differentiation (17). Moreover, it has been reported that WIN18,446 had no effect on serum testosterone concentration (66), indicating that the effects of WIN18,446 on spermatogenesis are not due to altered testosterone levels, but to the inhibition of RA signaling in the testes.

Identification of Meiotic Prophase Stages. Middle pachytene, late pachytene, and diplotene stages were identified according to the following criteria (35, 36, 38, 39, 67, 68): middle pachytene stage, completely synapsed autosomes as judged by staining for SYCP3, largely asynapsed XY chromosomes as judged by staining for SYCP3, beginning of H1t incorporation (low signal), and sex body formation as judged by staining for γH2AX and ATR; late pachytene stage, asynapsis of autosomal ends as judged by staining for SYCP3, unsynapsed XY chromosomes as judged by staining for SYCP3, high accumulation of H1t (high signal); diplotene stage, asynapsed autosomes as judged by staining for SYCP3. High H1t accumulation and the γH2AX and ATR signals seen on the sex body at late pachytene stage all persist to the diplotene stage.

Experimental Design to Synchronize Seminiferous Stages in Young Testes. Because Sertoli cells express an RA-synthesizing enzyme, aldehyde dehydrogenase 1A1 (*Aldh1a1*), Sertoli cells have been hypothesized to be a source of RA in the testes of young males (28, 42). Given that Sertoli cells proliferate in newborn males, with their numbers increasing until P12 to P14 (69, 70), changes in RA concentration in stage-synchronized testes might be due not only to changes in seminiferous stages but also to increasing numbers of Sertoli cells during postnatal development. To bypass the possible effects of such Sertoli cell proliferation, we injected mice with WIN18,446 daily from P2 until P14, by which point Sertoli cell proliferation has ceased (Fig. 5*A* and Fig. S5*A*).

After a single injection of RA into these WIN18,446-pretreated mice, the arrested germ cells undergo spermatogonial differentiation to initiate spermatogenesis in a highly synchronized manner. Spermatogenesis following this single RA injection is more synchronized than in the absence of RA injection, or in unperturbed young testes (the "first wave of spermatogenesis") (41). Accordingly, we gave daily injections of WIN18,446 from P2 until P14 and then injected a single dose of RA at P15 (Fig. 5*A*).

Although spermatogenesis in young testes proceeds more rapidly than in adult testes (33), we confirmed that the germ cell association patterns in young testes, which represent seminiferous stages, are consistent with those in adult testes (Fig. S5*B*). In addition, the expression patterns of an RA-responsive gene, STRA8, in young testes are also consistent with those in adult testes (22) (Fig. S5*C*). Taken together, we believe that changes in RA levels in young testes should reflect those in adult testes.

Depleted Cell Cohort After Successive HU Injections. Because the S phase and whole cell cycle of all differentiating spermatogonia (A_1/A_2/A_3/A_4/intermediate/B spermatogonia) last 7 to 18 h and 28 to 31 h, respectively (6, 46), these cells are completely depleted by six injections of HU at 6-h intervals (spanning a total of 30 h). By contrast, undifferentiated spermatogonia are only partially depleted because they have different cell cycle characteristics; undifferentiated spermatogonia in stages II to VIII are arrested in G0/G1 phase (1, 71), and proliferative undifferentiated spermatogonia in stages IX to I have a longer cell cycle than do differentiated spermatogonia (72, 73). Thus, at 36 h after the first HU injection, differentiating spermatogonia are completely absent whereas undifferentiated spermatogonia are still present in all seminiferous stages (46) (Fig. 5*C*).

Detection of Transcripts in smFISH Experiments. Because smFISH probes detect and localize each target mRNA molecule as a small punctate signal (47, 65), large spots can be recognized as nonspecific signals that are readily distinguished from punctate signals. When double smFISH staining with two different gene probes (green and red fluorescent probes) was performed, some autofluorescent spots were visualized, regardless of the gene probes employed, as yellow signals (merge of green and red) (Fig. 6*A* and Fig. S7 *A* and *B*). When quantifying the transcripts, these spots were automatically excluded from the analysis using custom Matlab software (47) (Fig. 6 *B*–*D* and Fig. S7 *C* and *D*). In smFISH-stained testes, round spermatids frequently displayed large single spots at their chromatoid bodies (Fig. 6*A* and Fig. S7 *A* and *B*). Because mRNAs stored in the chromatoid body are thought to be translationally repressed or decayed (74), we considered these spots to be nonspecific, or to represent nonfunctional mRNA signals. These spots were unlikely to be aggregated punctate signals, and the custom Matlab software employed did not recognize them as specific signals (Fig. 6 *B*–*D*). Moreover, some probes for *Stra8*, which is not expressed in spermatids (20), also detected large spots at the chromatoid body, suggesting that these spots do not represent specific (or functional) mRNA transcripts. Our smFISH results for *Stra8* (Fig. S7 *A*–*C*) were consistent with the previously reported pattern of *Stra8* mRNA (and protein) expression (21, 22).

We rarely detected *Aldh1a3* transcripts in either germ cells or Sertoli cells (Fig. 6 *A* and *D*). As a positive control, we tested for and observed *Aldh1a3* signals in young kidneys (75) (Fig. S7 *E* and *F*), confirming the specificity and sensitivity of our smFISH probes for *Aldh1a3*. We conclude that *Aldh1a3* expression is very low or absent in both germ cells and Sertoli cells. Overall, the patterns of mRNA expression that we observed for *Aldh1a1-3* in control seminiferous tubules were consistent with previous reports (42, 43).

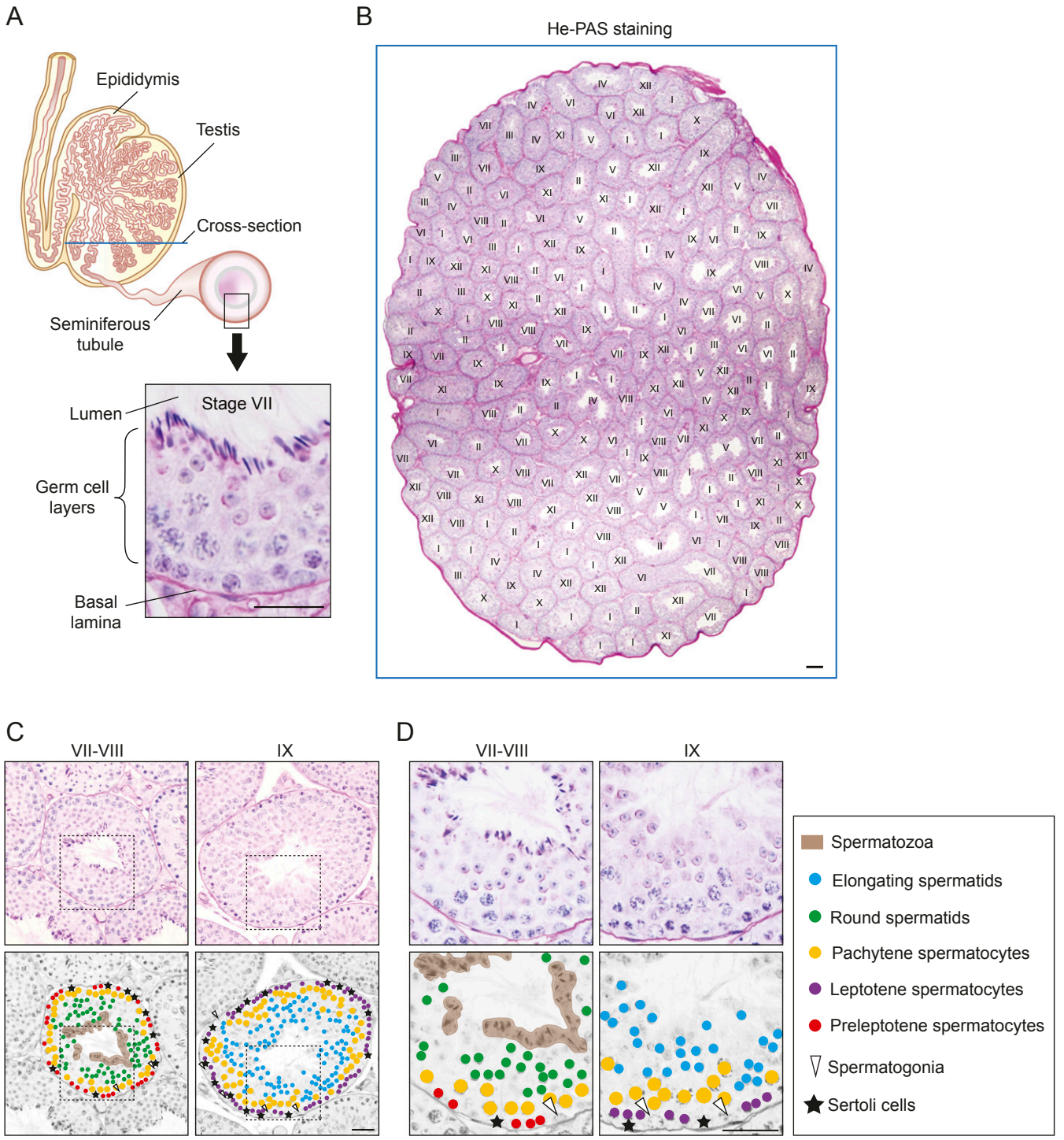

Fig. S1. Overview of mouse spermatogenesis. (*A*) Structure of the mouse testis comprising seminiferous tubules. In any given tubule cross-section, one observes germ cells at different steps of their development into spermatozoa. These germ cell types are concentrically layered; undifferentiated spermatogonia lie on the basal lamina of the tubule, and germ cells move toward the tubule lumen as they differentiate (10). Germ cell differentiation is precisely timed; hence, particular steps of development are always found together at the same time and place (Fig. 1). The blue line indicates the orientation of testis cross-sections in *B*. (*Lower*) A representative tubule cross-section in stage VII, stained with hematoxylin and periodic acid-Schiff (He-PAS). Adapted from ref. 22. (Scale bar: 30 μm.) (*B*) A representative testis cross-section, stained with He-PAS. Reused from ref. 22. (Scale bar: 100 μm.) (*C* and *D*) (*Top*) Representative tubule cross-sections in stages VII and VIII and stage IX, stained with He-PAS. (*Bottom*) Grayscale versions of *Top* panels. Boxed regions (98.7 μm × 98.7 μm) in *C* (245 μm × 245 μm) indicate areas shown in higher magnification in *D*. Stars, Sertoli cells; white arrowheads, spermatogonia; dots, preleptotene (red) spermatocytes, leptotene spermatocytes (purple), pachytene spermatocytes (yellow), step 7 and 8 round spermatids (green), and step 9 elongating spermatids (blue). Brown areas, spermatozoa. (Scale bar: 30 μm.)

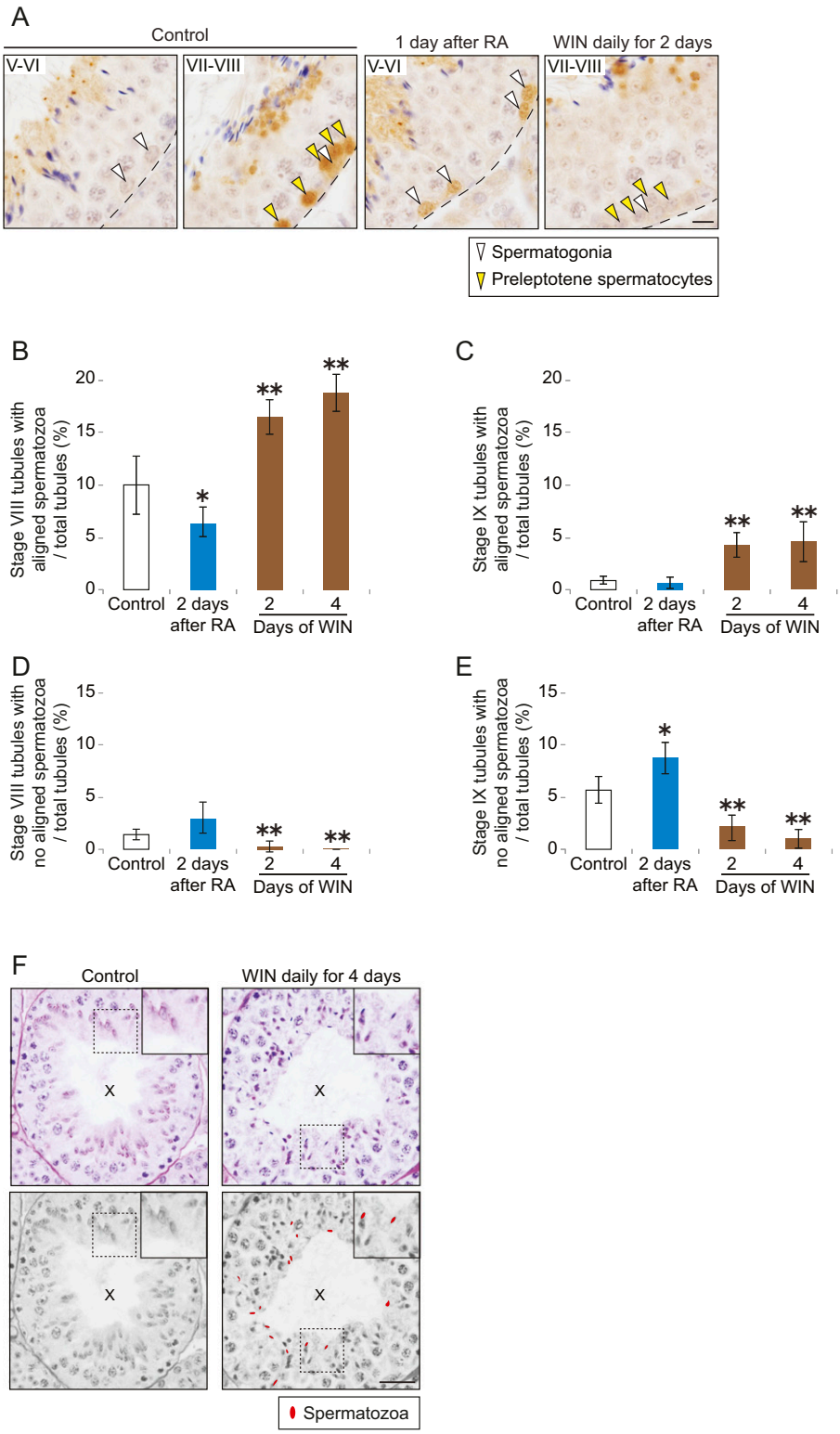

Fig. S2. RA injection induces, and WIN18,446 injection inhibits, the release of spermatozoa. (*A*) Immunostaining for STRA8 on testis cross-sections in controls, 1 d after a single RA injection, and after 2 d of daily WIN18,446 injections. Roman numerals indicate stages. Dashed lines, basal laminae of tubule cross-sections; arrowheads, spermatogonia (white) and preleptotene spermatocytes (yellow). (Scale bar: 10 μm.) (*B* and *C*) Number of stage VIII (*B*) or stage IX (*C*) tubule cross-sections with aligned spermatozoa per total tubule cross-sections, in controls, or 2 d after a single RA injection, or after 2 or 4 d of daily WIN18,446 injections. Error bars, mean ± SD, $*P < 0.05$, $**P < 0.01$, compared with control (one-tailed *t* test). (*D* and *E*) Number of stage VIII (*D*) or stage IX (*E*) tubule cross-sections with no aligned spermatozoa per total tubule cross-sections, in controls, or 2 d after a single RA injection, or after 2 or 4 d of daily WIN18,446 injections. Error bars, mean ± SD, $*P < 0.05$, $**P < 0.01$, compared with control (one-tailed *t* test). (*F*, *Top*) Control (*Left*) and WIN18,446-injected (*Right*) testis cross-sections in stage X, stained with hematoxylin and periodic acid-Schiff (He-PAS). (*F*, *Bottom*) Grayscale versions of top panels. *Insets* (36.4 μm × 36.4 μm) enlarge the boxed regions. Red dots, spermatozoa. (Scale bar: 30 μm.)

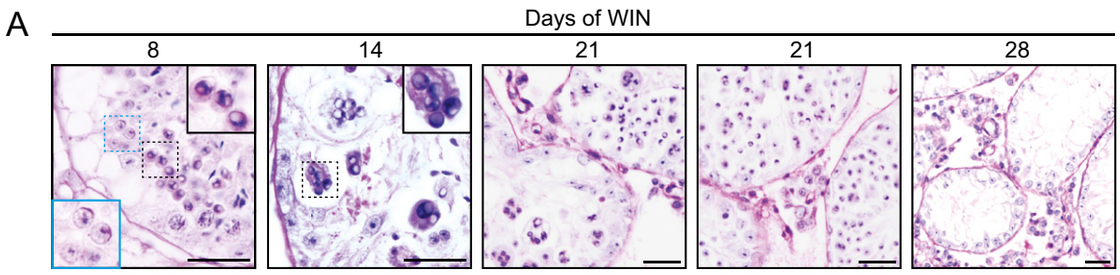

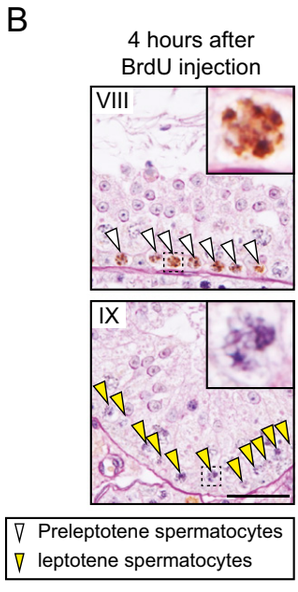

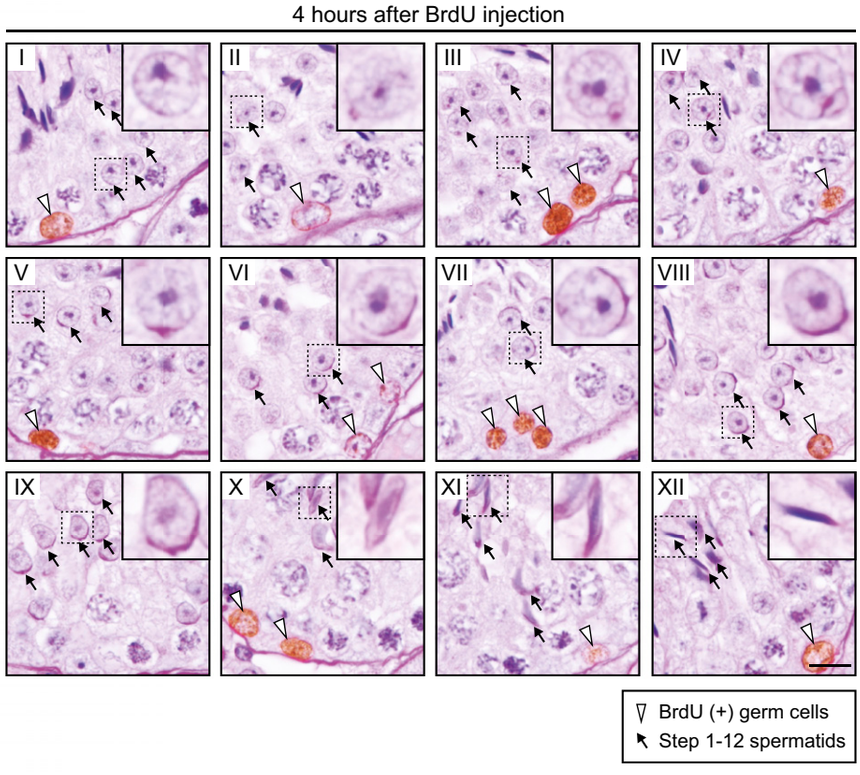

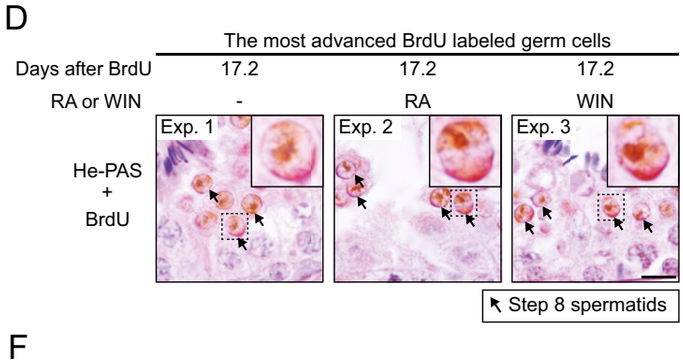

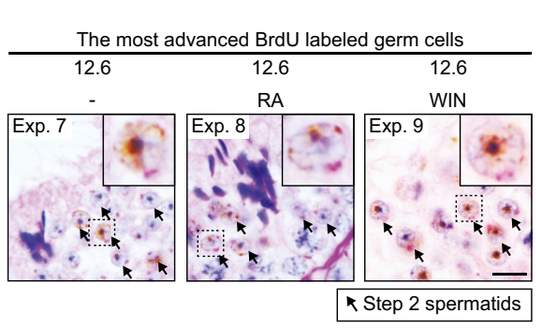

F

Days after BrdU	Treatment	Step 2		Step 8		Step 9		Step 10		Step 11	
		Tubules counted	BrdU+ Tubules (%)	Tubules counted	BrdU+ tubules (%)	Tubules counted	BrdU+ tubules (%)	Tubules counted	BrdU+ tubules (%)	Tubules counted	BrdU+ tubules (%)
12.6	Cont	32	15 (46.9)	n.d.		n.d.		n.d.		n.d.	
12.6	RA	30	14 (46.7)	n.d.		n.d.		n.d.		n.d.	
12.6	WIN	31	14 (45.2)	n.d.		n.d.		n.d.		n.d.	
17.2	Cont	n.d.		39	22 (56.4)	n.d.		n.d.		n.d.	
17.2	RA	n.d.		47	26 (55.3)	n.d.		n.d.		n.d.	
17.2	WIN	n.d.		66	36 (54.5)	n.d.		n.d.		n.d.	
18.2	Cont	n.d.		n.d.		27	17 (63.0)[a,b]	41	35 (85.4)[a]	31	0 (0)[b]
18.2	RA	n.d.		n.d.		19	11 (57.9)[a]	20	17 (85.0)[a]	83	63 (75.9)[a]
18.2	WIN	n.d.		n.d.		15	14 (93.3)[b]	6	0 (0)[b]	80	0 (0)[b]

Fig. S3. RA promotes initiation of spermatid elongation but not meiotic progression. (*A*) WIN18,446-injected testis cross-sections, stained with hematoxylin and periodic acid-Schiff (He-PAS). Mice were given daily s.c. injections of WIN18,446 for 8 d, 14 d, 21 d, or 28 d. *Insets* (17 μm × 17 μm) enlarge the boxed regions containing normal step 7 and 8 (blue box) and apoptotic (black box) round spermatids. The sections at 8 d and 14 d also contained unreleased spermatozoa. At 21 d, nearly all tubules containing spermatids showed complete block of spermatid elongation, and resultant apoptosis. At 28 d, seminiferous tubules contained only type A spermatogonia and Sertoli cells, as others have observed in vitamin A-deficient mice (17). (Scale bars: 30 μm.) (*B*) The most advanced BrdU-labeled germ cells in control testis cross-sections 4 h after a single BrdU injection, immunostained for BrdU with He-PAS staining. Roman numerals indicate stages. *Insets* (9.1 μm × 9.1 μm) enlarge the boxed regions. Arrowheads, BrdU-positive preleptotene (white) and BrdU-negative leptotene (yellow) spermatocytes. (Scale bar: 30 μm.) (*C*) Representative BrdU-positive germ cells and BrdU-negative spermatids in control testis cross-sections 4 h after a single BrdU injection, immunostained for BrdU with He-PAS staining. Roman numerals indicate stages. *Insets* (stages I to X, 7.5 μm × 7.5 μm; stages XI and XII, 9.8 μm × 9.8 μm) enlarge the boxed regions. Arrowheads, BrdU-positive germ cells. Arrows, step 1 to 12 spermatids. (Scale bar: 10 μm.) (*D* and *E*) The most advanced BrdU-labeled germ cells in testis cross-sections of control (*Left*), RA-injected (*Middle*), or WIN18,446-injected (*Right*) mice 17.2 d (*D*; Exps. 1 to 3 in Fig. 3*C*) or 12.6 d (*E*; Exps. 7 to 9 in Fig. 3*C*) after a single BrdU injection, immunostained for BrdU and hematoxylin and periodic acid-Schiff (He-PAS) staining. *Insets* (7.5 μm × 7.5 μm) enlarge the boxed regions. Arrows in *D*, step 8 spermatids; arrows in *E*, step 2 spermatids. (Scale bars: 10 μm.) (*F*) Number and percentage of tubules containing BrdU-labeled spermatids (step 2, 8, 9,10, or 11) in testis cross-sections. n.d., not determined. Percentages of tubules containing the most advanced BrdU$^+$ spermatids did not differ significantly among control, RA-treated, and WIN18,446-treated groups 12.6 d (*E*; Exps. 7 to 9 in Fig. 3*C*) or 17.2 d (*D*; Exps. 1 to 3 in Fig. 3*C*) after a single BrdU injection (three or four biological replicates; $P > 0.05$; χ^2 test). a and b, Data with different superscripts in the same column differ significantly among control, RA-treated, and WIN18,446-treated groups 18.2 d (Fig. 3*D*; Exps. 4 to 6 in Fig. 3*C*) after a single BrdU injection (three or four biological replicates; $P < 0.05$; Fisher's exact test).

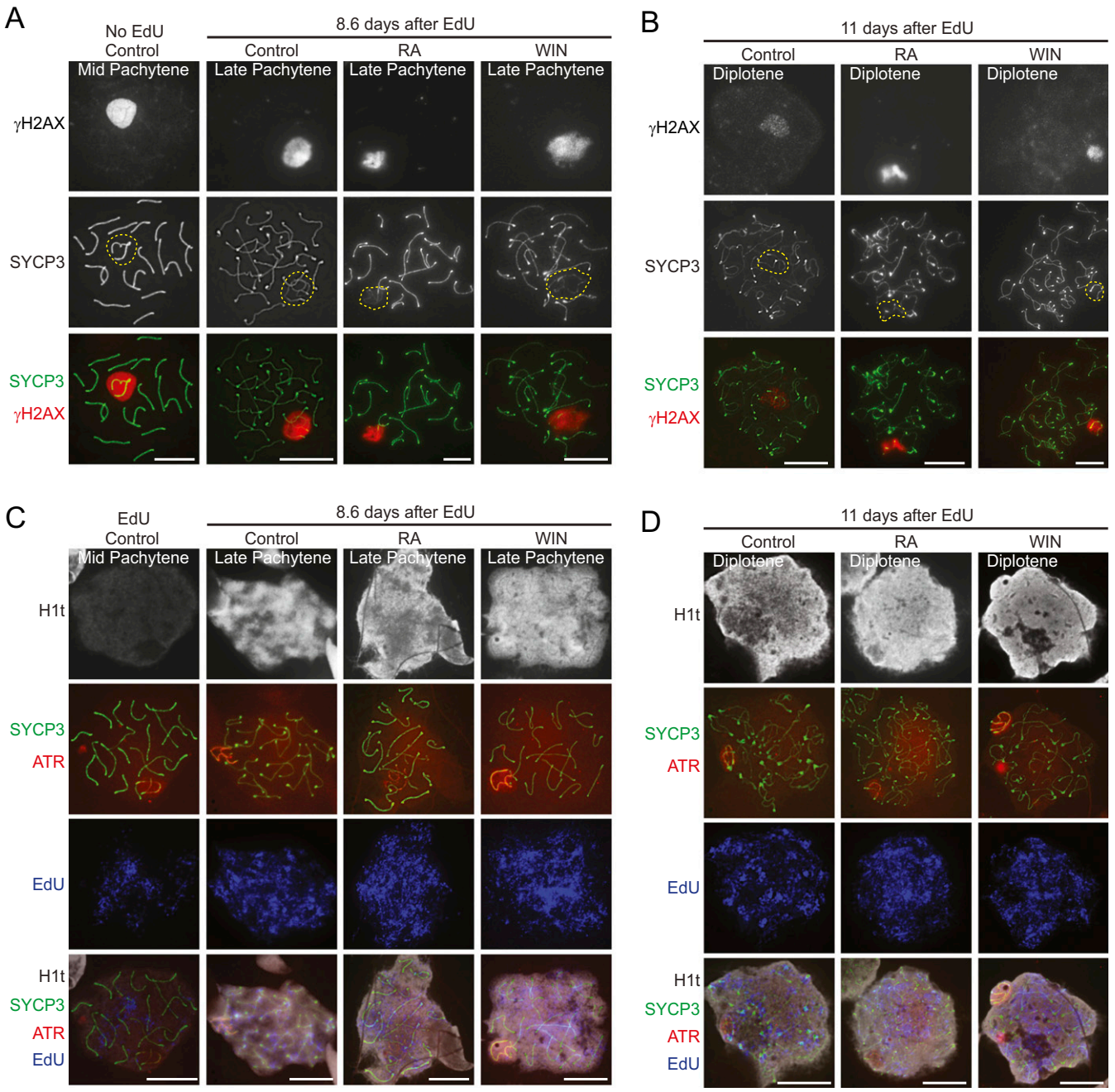

Fig. S4. RA has no discernible effect on meiotic progression. (*A* and *B*) The most advanced EdU-labeled germ cells in nuclear spreads of spermatocytes in control or daily RA- or WIN18,446-injected mice at 8.6 d (*A*; late pachytene stage) or 11 d (*B*; diplotene stage) after a single EdU injection, immunostained for SYCP3 (green) and γH2AX (red), shown in Fig. 4 (SYCP3 and γH2AX merged panels are duplicated from Fig. 4). SYCP3 and γH2AX images were separated to visualize SYCP3 localization on segregating sex chromosomes. Yellow dashed lines in SYCP3 panels encircle γH2AX-localized areas, which are predicted to be XY bodies. (*A*, *Far Left*) A representative mid-pachytene spermatocyte showing no EdU signal in controls. (Scale bars: 10 μm.) (*C* and *D*) The most advanced EdU-labeled germ cells in nuclear spreads of spermatocytes in control or daily RA- or WIN18,446-injected mice at 8.6 d (*C*; late pachytene stage) or 11 d (*D*; diplotene stage) after a single EdU injection, immunostained for H1t (gray), SYCP3 (green), ATR (red), and EdU (blue). (*C*, *Far-Left*) A representative mid-pachytene spermatocyte showing EdU-positive signal in controls. (Scale bars: 10 μm.)

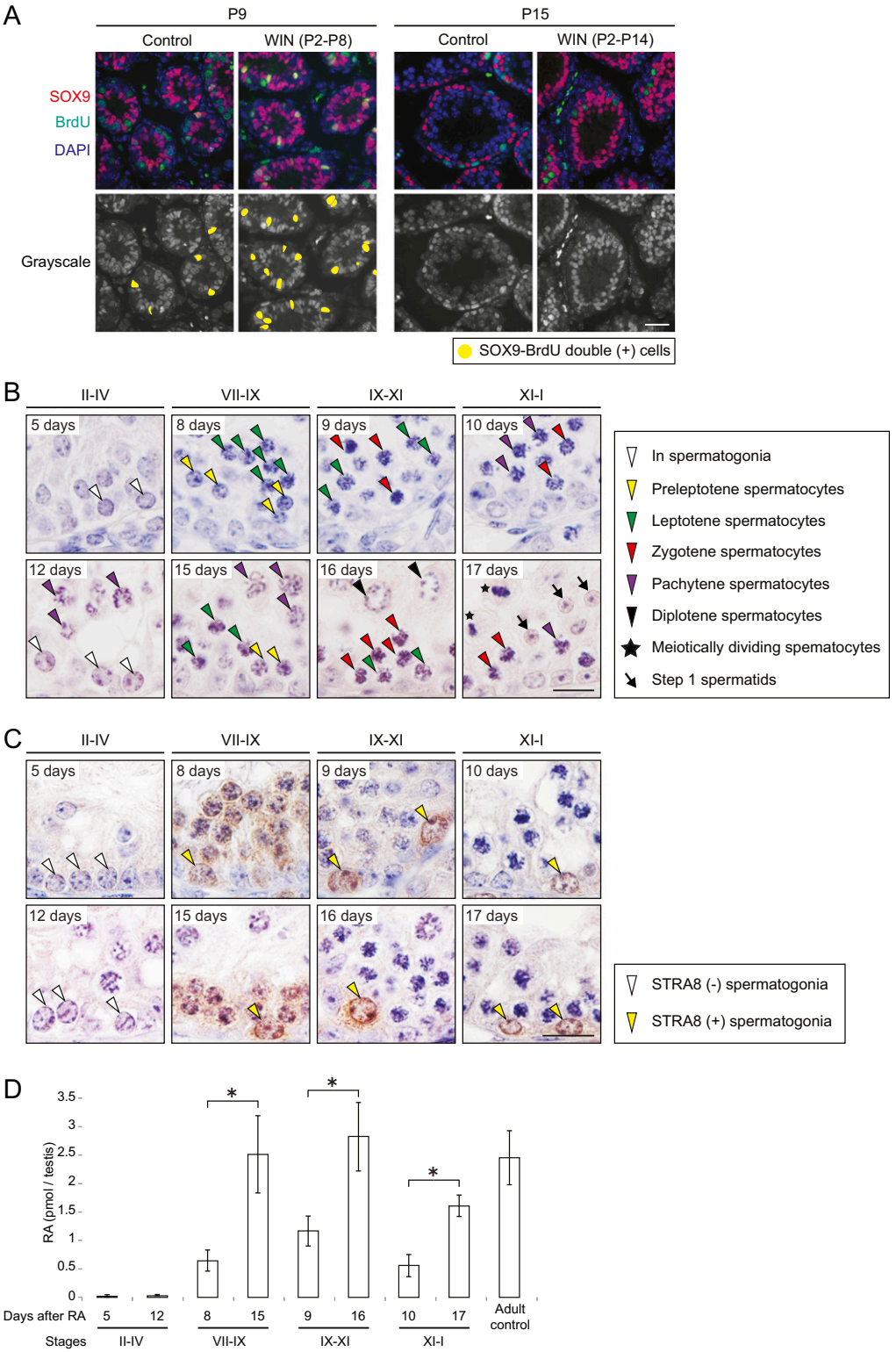

Fig. S5. RA concentrations change periodically in stage-synchronized testes of WIN18,446/RA-injected young males. (*A*, *Top*) Immunostaining for a Sertoli cell nucleus specific marker, SOX9 (red), and BrdU (green), with DAPI counterstain, in testis cross-sections of control and WIN18,446-injected mice at postnatal day 9 (P9) and P15. Mice were given daily injections of WIN18,446 from P2 until P8 or P14. (*A*, *Bottom*) Grayscale versions of *Top* panels. Yellow-labeled cells, SOX9-BrdU double-positive cells. (Scale bar: 30 μm.) (*B*) Representative tubule cross-sections in synchronized (WIN18,446/RA-injected) young testes, stained with hematoxylin. Mice were given daily injections of WIN18,446 from postnatal day 2 (P2) until P14 and were then given a single dose of RA at P15. Testes were harvested at the indicated days (in panels) after RA injection. Roman numerals indicate stages. Arrowheads, intermediate spermatogonia (white) and preleptotene (yellow), leptotene (green), zygotene (red), pachytene (purple), and diplotene (black) spermatocytes. Stars, meiotically dividing spermatocytes. Arrows, step 1 spermatids. (Scale bar: 10 μm.) (*C*) Immunostaining for STRA8 on testis cross-sections in synchronized (WIN18,446/RA-injected) young testes. Roman numerals indicate stages. Arrowheads, STRA8-negative (white) and STRA8-positive (yellow) spermatogonia. (Scale bar: 10 μm.) (*D*) Absolute quantification of RA levels (pmol per testes) in synchronized (WIN18,446/RA-injected) young testes. Bar graphs at 12, 15, 16, and 17 d after RA injection show the results from two biological replicates. Error bars, mean ± SD, $*P < 0.01$ (one-tailed *t* test).

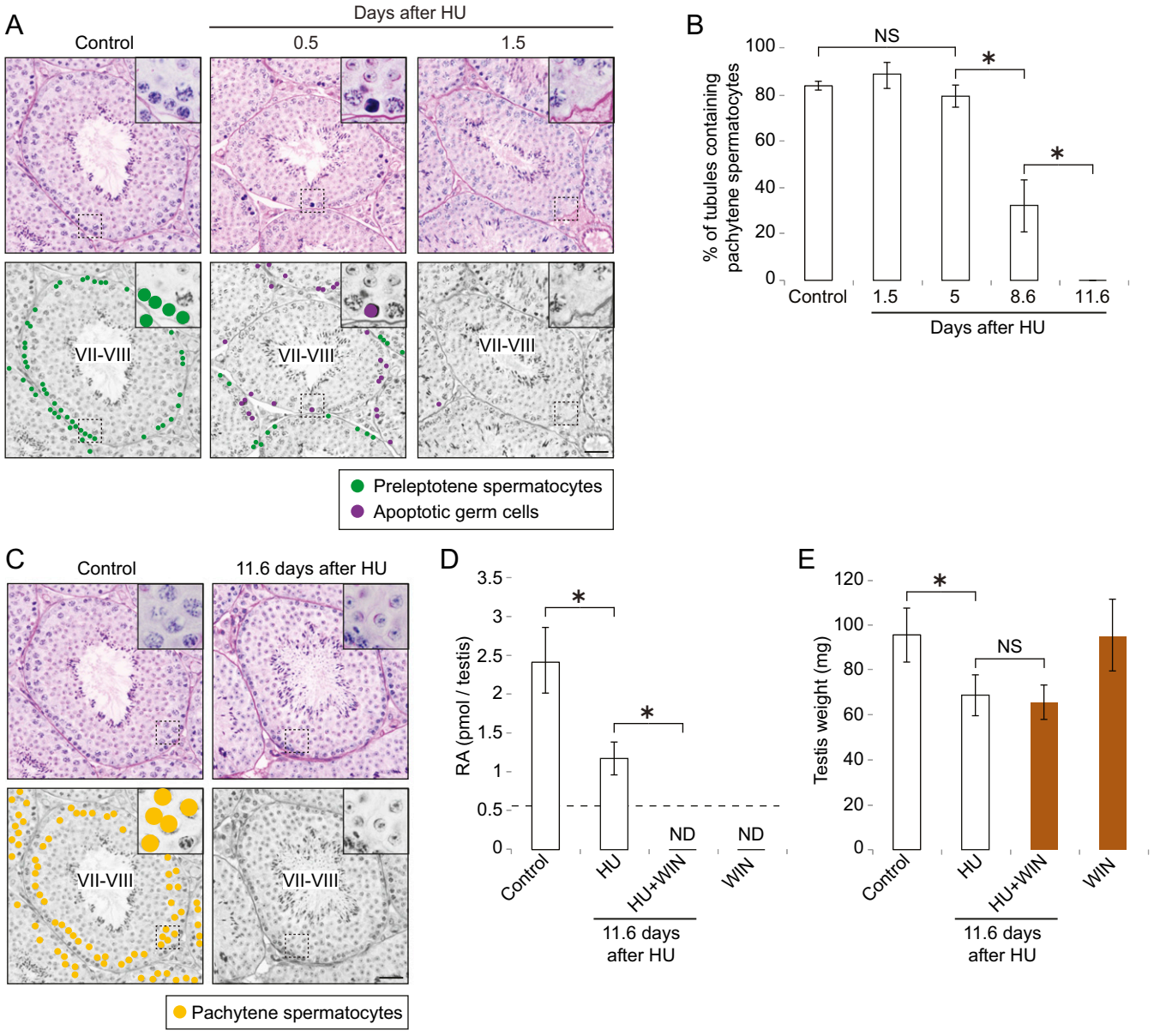

Fig. S6. Depletion of pachytene spermatocytes reduces RA concentration in testes. (*A*, *Top*) Control and HU-injected testis cross-sections in stages VII and VIII, stained with hematoxylin and periodic acid-Schiff (He-PAS). Mice received injections of HU at 6-h intervals, and testes were collected 12 h (0.5 d) or 36 h (1.5 d) after the first HU injection ("Control" panel is duplicated from Fig. 5*D*). (*A*, *Bottom*) Grayscale versions of *Top* panels. *Insets* (28.5 μm × 28.5 μm) enlarge the boxed regions. Dots, preleptotene spermatocytes (green) and apoptotic germ cells (purple). (Scale bar: 30 μm.) (*B*) Percentage of tubule cross-sections containing pachytene spermatocytes, in controls and 1.5, 5, 8.6, and 11.6 d after the first HU injection. At 8.6 d, pachytene spermatocytes in stages I to VII were depleted. Error bars, mean ± SD, $*P < 0.01$ (Tukey–Kramer test). NS, not significant ($P > 0.05$). (*C*, *Top*) Testis cross-sections in stages VII and VIII of control and HU-injected mice, stained with He-PAS, as also shown in Fig. 5*D* ("Control" and HU-injected panels are duplicated from Fig. 5*D*) (*C*, *Bottom*) Grayscale versions of *Top* panels. Orange dots, pachytene spermatocytes. *Insets* (28.5 μm × 28.5 μm) enlarge the boxed regions. (Scale bar: 30 μm.) (*D* and *E*) Absolute quantification of RA levels (pmol per testes) (*D*) and testis weights (mg) (*E*) in control and HU-injected adult testes. Testis weight declined at 11.6 d after the first HU injection because of the absence of pachytene spermatocytes. HU + WIN, mice were given injections of HU and then daily injections of WIN18,446, beginning 7.6 d after the first HU injection. WIN, mice received daily injections of WIN18,446 for 4 d. Dashed line, limit of detection. ND, not detected (below the limit of detection). The far right "WIN" bar graph in *D* shows the results from two biological replicates. Error bars, mean ± SD, $*P < 0.01$ (Tukey–Kramer test). NS, not significant ($P > 0.05$).

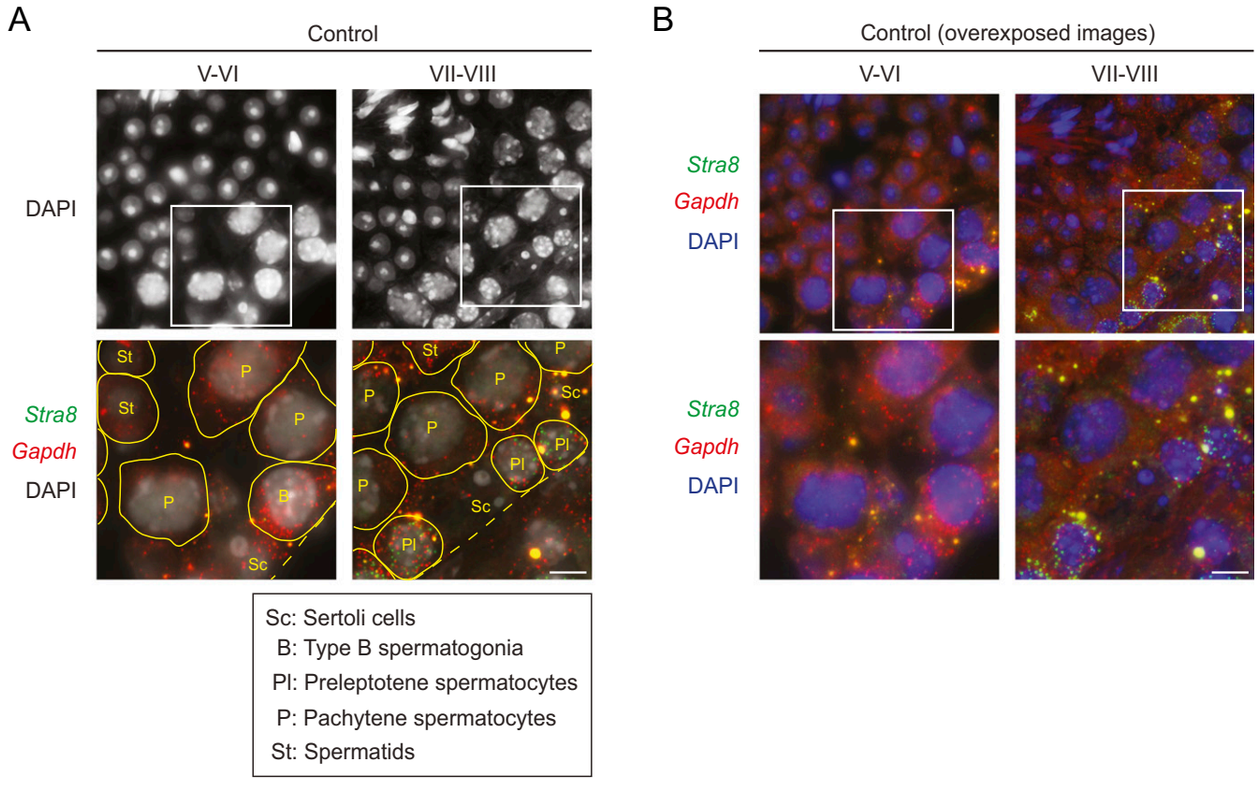

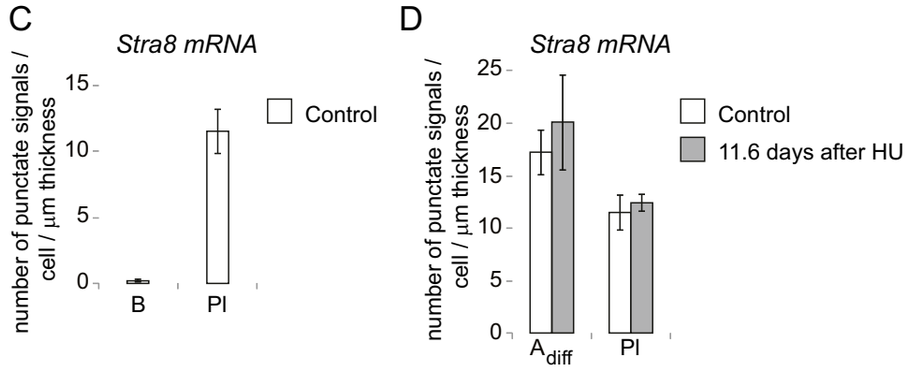

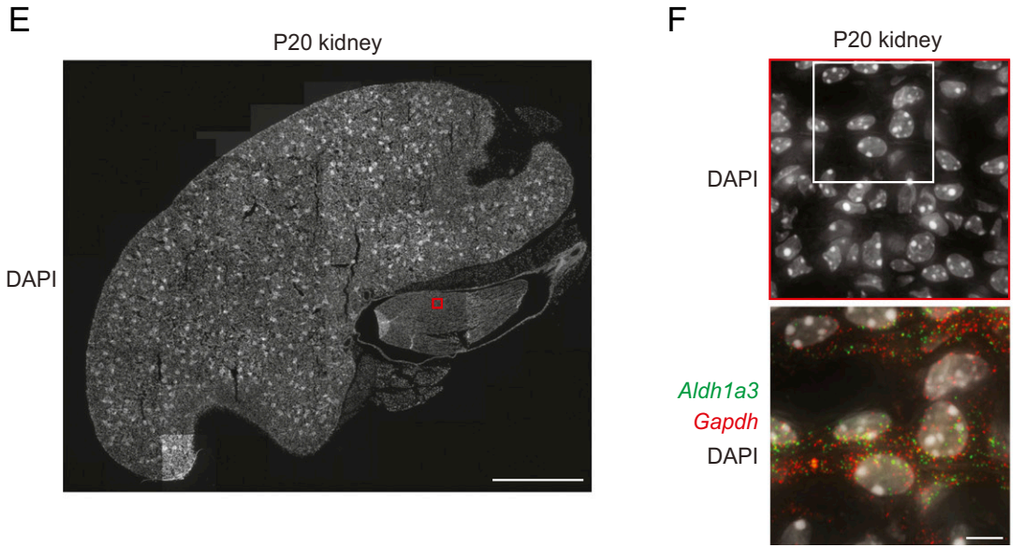

Fig. S7. Depletion of pachytene spermatocytes has no effect on *Stra8* mRNA expression. (*A*) Single molecule fluorescence in situ hybridization (smFISH) for mRNAs of *Stra8* (green) and *Gapdh* (red), with DAPI counterstain (gray), on control testis cross-sections in stages V and VI and in stages VII and VIII. Single transcripts are visible as punctate signals. Large spots in round spermatids are nonspecific signals (SI Results). Yellow spots in merged images are autofluorescent signals. Boxed regions (32.5 μm × 32.5 μm) in DAPI images (65 μm × 65 μm) indicate areas shown in higher magnification below each image. Yellow lines encircle germ cells, according to the cell borders visualized by overexposed images in *B*. B, type B spermatogonia; dashed lines, basal laminae of tubule cross-sections; Pl and P, preleptotene and pachytene spermatocytes; Sc, Sertoli cells; St, spermatids. (Scale bar: 5 μm.) (*B*) Overexposed images of smFISH for mRNAs of *Stra8* (green) and *Gapdh* (red), with DAPI counterstain (blue), in control testis cross-sections in stages V and VI and in stages VII and VIII, shown in *A*. Boxed regions (32.5 μm × 32.5 μm) in *Upper* images (65 μm × 65 μm) indicate areas shown in higher magnification below each image. (Scale bar: 5 μm.) (*C*) Number of smFISH punctate signals per cell per 1-μm section thickness for *Stra8* mRNA, in cross-sections of control tubules at stages V to VIII. Error bars, mean ± SE. B, type B spermatogonia; Pl, preleptotene spermatocytes. (*D*) Number of smFISH punctate signals per cell per 1-μm section thickness for *Stra8* mRNA, in controls or 11.6 d after the first HU injections, in stages VII and VIII. Error bars, mean ± SE. A_{diff}, differentiating type A spermatogonia; Pl, preleptotene spermatocytes. (*E*) Representative control kidney cross-section at postnatal day 20 (P20), stained with DAPI (gray). Individual images are stitched together for an entire P20 kidney. Red boxed region indicates area shown in higher magnification in *F*. (Scale bar: 1 mm.) (*F*) smFISH for mRNAs of *Aldh1a3* (green) and *Gapdh* (red), with DAPI counterstain (gray), on control kidney cross-sections as a positive control tissue for *Aldh1a3* expression. White boxed region (32.5 μm × 32.5 μm) in DAPI image (65 μm × 65 μm) indicates area shown in higher magnification *Below*. (Scale bar: 5 μm.)

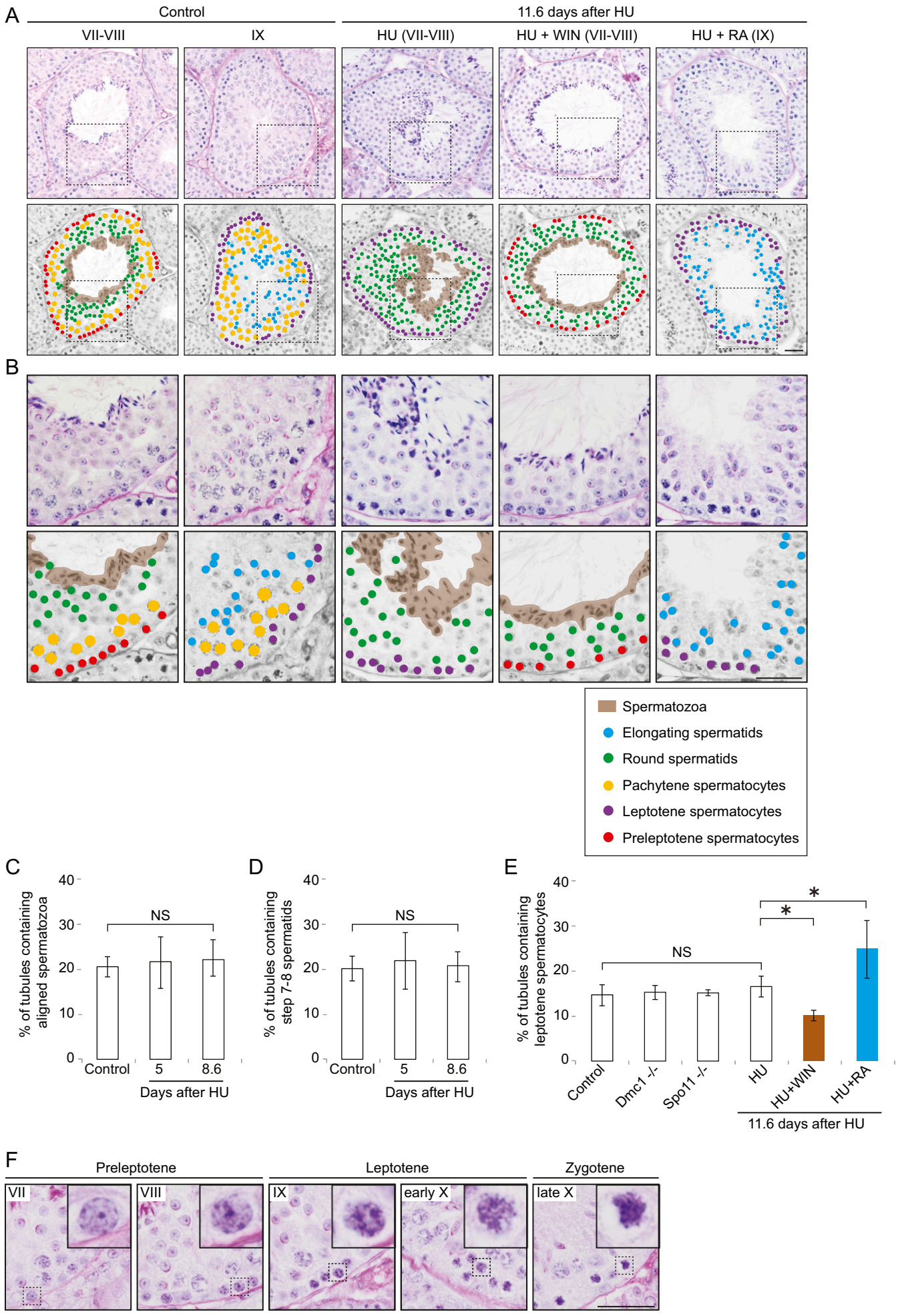

Fig. S8. RA from pachytene spermatocytes is required for postmeiotic but not for premeiotic transitions. (*A* and *B*) (*Top*) Representative tubule cross-sections in controls and 11.6 d after the first HU injection, stained with hematoxylin and periodic acid-Schiff (He-PAS). Roman numerals indicate stages. HU + WIN, mice were given injections of HU and were then given daily injections of WIN18,446, beginning 7.6 d after the first HU injection. HU + RA, mice received a single dose of RA, 9.6 d after the first HU injection. (*Bottom*) Grayscale versions of *Top* panels. Boxed regions (98.7 μm × 98.7 μm) in *A* (245 μm × 245 μm) indicate areas shown in higher magnification in *B*. Stars, Sertoli cells; dots, preleptotene spermatocytes (red), leptotene spermatocytes (purple), pachytene spermatocytes (yellow), round spermatids (green), and elongating spermatids (blue). Brown areas, spermatozoa. (Scale bars: 30 μm.) Some HU-treated tubules include (unreleased) aligned spermatozoa, (unelongated) step 7 and 8 spermatids, and (meiotic) leptotene spermatocytes. This unusual combination of spermatogenic cell types is expected if, as we argue, elimination of pachytene-derived RA (via HU treatment) inhibits sperm release and spermatid elongation but does not affect meiotic initiation. Tubules that contain step 7 and 8 spermatids are, by convention, identified as stage VII and VIII tubules (10). (*C* and *D*) Percentage of testis tubule cross-sections containing aligned spermatozoa (*C*) or step 7 and 8 spermatids (*D*), in controls or 5 or 8.6 d after the first HU injection. No accumulations of aligned spermatozoa or step 7 and 8 spermatids were observed at these time points, when *Aldh1a2*-expressing pachytene and diplotene spermatocytes had not yet been depleted (Fig. 5*C* and Fig. S6*B*). This result suggests that the accumulations observed at 11.6 d were not due to cytotoxic effects of HU on aligned spermatozoa or step 7 and 8 spermatids. Error bars, mean ± SD. NS, not significant ($P > 0.05$; Tukey–Kramer test). (*E*) Depletion of pachytene spermatocytes has no effect on meiotic initiation. Percentage of testis tubule cross-sections containing leptotene spermatocytes, in controls or 11.6 d after the first HU injection, and in *Dmc1*- or *Spo11*-deficient testes. Error bars, mean ± SD, *$P < 0.05$ (Tukey–Kramer test). NS, not significant ($P > 0.05$). (*F*) Representative images of preleptotene, leptotene, and zygotene spermatocytes in stages VII to X of control testis cross-sections. These germ cell types were identified by their distinctive nuclear morphologies (62). Preleptotene stage, a rim of chromatin lines the inner nuclear envelope, and chromatin patches are found along the nuclear envelope. Leptotene stage, the nucleus lacks peripheral chromatin and instead exhibits fine chromatin threads. Zygotene stage, the filaments of chromosomes appear thicker than those of leptotene cells, and the nucleus is usually notched. *Insets* (9.1 μm × 9.1 μm) enlarge the boxed regions. (Scale bar: 30 μm.)

Other Supporting Information Files

Dataset S1 (XLSX)
Dataset S2 (XLSX)